

**Speciation and decomposition pathways of ruthenium catalysts used for selective C–H hydroxylation**

Journal:	<i>Chemical Science</i>
Manuscript ID:	SC-EDG-04-2014-001050.R1
Article Type:	Edge Article
Date Submitted by the Author:	22-May-2014
Complete List of Authors:	Flender, Cornelia; Stanford University, Chemistry Adams, Ashley; Stanford University, Chemistry Roizen, Jennifer; Duke University, Chemistry McNeill, Eric; Harvard University, Chemistry and Chemical Biology Du Bois, Justin; Stanford University, Department of Chemistry Zare, Richard; Stanford University, Chemistry

ARTICLE

Speciation and decomposition pathways of ruthenium catalysts used for selective C–H hydroxylation

Cite this: DOI: 10.1039/x0xx00000x

Cornelia Flender, Ashley M. Adams, Jennifer L. Roizen[†], Eric McNeill, J. Du Bois* and Richard N. Zare*

Received 00th January 2012,
Accepted 00th January 2012

DOI: 10.1039/x0xx00000x

www.rsc.org/

Mechanistic insight into a C–H hydroxylation reaction catalysed by $[(\text{Me}_3\text{tacn})\text{RuCl}_3]$ has been obtained using desorption electrospray ionization mass spectrometry (DESI-MS) to identify reactive intermediates and to determine that fate of the starting metal complex. Our studies provide direct evidence for the formation of a high-valent dioxo-Ru(VI) species, which is believed to be the active oxidant. Other unexpected Ru-oxo intermediates, however, have been identified and may also function as competent hydroxylating agents. Mass spectral data that substantiate putative mechanisms for catalyst arrest and highlight reactivity differences between $[(\text{Me}_3\text{tacn})\text{RuCl}_3]$ and the corresponding tribromide adduct are also described.

Introduction

The hydroxylation of unactivated C–H bonds remains a leading challenge in modern organic chemistry despite recent, notable advances using both metal- and nonmetal-based catalysts to effect this transformation.^{1,2,3,4} Following earlier work of Che, we have demonstrated the utility of (1,4,7-trimethyl-1,4,7-triazacyclononane)ruthenium(III) trichloride ($[(\text{Me}_3\text{tacn})\text{RuCl}_3]$, **1**) for oxidation of tertiary and certain benzylic C–H bonds on substrates of varying complexities (Figure 1).⁵ Under optimized conditions, this reaction is conducted in aqueous solution using either ceric ammonium nitrate (CAN) or sodium periodate (NaIO_4) as the stoichiometric oxidant. Mechanistic evidence, including both substrate selectivity and kinetic isotope effect data, suggest that oxidation occurs by an initial C–H abstraction event followed by fast, solvent-caged radical rebound. In order to gain additional insight into the reaction process and the mechanism(s) for catalyst arrest, we have utilized desorption electrospray ionization (DESI) coupled to mass spectrometry (MS)⁶ to detect transient reaction intermediates and catalyst-derived products. These experiments have revealed three oxo-substituted Ru species, including the putative active oxidant, a dioxo-Ru(VI) Me_3tacn adduct; mono-oxo Ru(IV) and dioxo-Ru(V) adducts have also been identified by DESI-MS. Examination of DESI-MS from spent reaction mixtures suggests possible mechanisms for inhibition of reaction turnover. Collectively, these results underscore the utility of DESI-MS as an analytical method for reaction methods development.⁷

Using DESI-MS, molecular ions corresponding to reaction intermediates with millisecond lifetimes can be detected.⁸ The detection of such fleeting species is achieved by spraying charged droplets of a reagent with the assistance of a nebulizing gas onto a

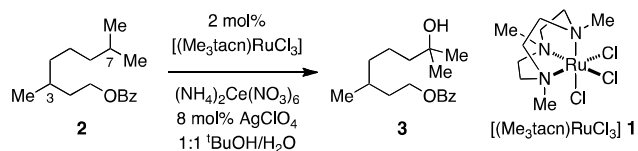


Figure 1. Tertiary C–H bond hydroxylation under Ru-catalysis.

sample that is spotted on a surface (Figure S1). Upon impact of the reagent and the sample, secondary droplets that contain the reaction partners are desorbed from the surface and directed into the MS for analysis. The reaction is initiated at the time the reagent droplets hit the sample on the surface, and continues inside these secondary droplets. Evaporation of the droplets takes place inside the transfer capillary of the MS to give the desolvated ions. The close spatial proximity of the microdroplet source to the MS inlet capillary allows for very short mixing times.⁹ In this study, we used DESI-MS to look at early time points of the $[(\text{Me}_3\text{tacn})\text{RuCl}_3]$ -catalysed C–H hydroxylation reaction. The distinct isotope profile of ruthenium and the high mass accuracy of an Orbitrap mass spectrometer¹⁰ allow for accurate identification of reaction products.

Results and Discussion

A. High-valent Ru oxidants. The oxidation of tertiary and benzylic C–H bonds mediated by catalytic amounts of $[(\text{Me}_3\text{tacn})\text{RuCl}_3]$ **1** proceeds smoothly in an aqueous alcohol solvent mixture, and either tertiary alcohol or ketone products can be obtained in synthetically useful yields (45–82%). In general, CAN proves to be the most effective as a terminal oxidant for this transformation.¹¹ The addition of a chloride scavenger, AgClO_4 , improves turnover number and overall product yields. The Ag(I) source is presumed to dissociate

the Cl^- groups from the $[(\text{Me}_3\text{tacn})\text{RuCl}_3]$ complex prior to the addition of oxidant. Initial DESI-MS studies, therefore, began by assessing the efficiency of this pre-incubation procedure. Catalyst **1** was treated with 4 equiv of AgClO_4 , the solution filtered and spotted on a paper surface for DESI analysis (Figure 2, top). In the mass spectrum, the most abundant signal corresponds to a molecular formula $[\text{LRuO}_2\text{H}_3\text{Cl}]^+$ ($\text{L} = \text{Me}_3\text{tacn}$). This finding demonstrates that the removal of a three chloride ligands by AgClO_4 is not complete prior to the addition of oxidant.

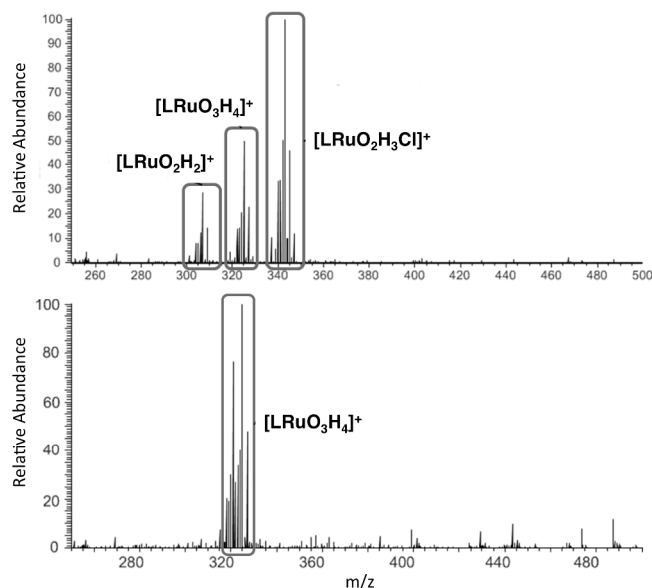


Figure 2. DESI spectra of $[(\text{Me}_3\text{tacn})\text{RuCl}_3]$ (top) and $[(\text{Me}_3\text{tacn})\text{RuBr}_3]$ (bottom) both incubated with AgClO_4 .

Our initial finding from the DESI-MS that AgClO_4 did not effect complete dissociation of chloride ligands prompted us to synthesize the corresponding tribromide complex, $[(\text{Me}_3\text{tacn})\text{RuBr}_3]$. Analysis of this catalyst prior to treatment with Ag(I) reveals three major forms, $[\text{LRuOBr}_2\text{H}]^+$, $[\text{LRuO}_2\text{BrH}_2]^+$ and $[\text{LRuO}_3\text{H}_3]^+$ with $[\text{LRuO}_2\text{BrH}_2]^+$ as the primary component (Figure S2). This finding contrasts analogous data with $[(\text{Me}_3\text{tacn})\text{RuCl}_3]$, a complex that exists in solution almost exclusively as the tris-chloride adduct (Figure S3). DESI analysis of $[(\text{Me}_3\text{tacn})\text{RuBr}_3]$ following treatment with AgClO_4 shows $[\text{LRuO}_3\text{H}_4]^+$ as the only Ru-containing species in the spectrum (Figure 2, bottom). From these data, it is evident that the bromide ligand is considerably more labile than its chloride counterpart.

DESI-MS of the reaction of $[(\text{Me}_3\text{tacn})\text{RuCl}_3]$ with substrate **2** and NaIO_4 shows a cationic ruthenium (VI) complex as the major Ru-containing analyte, which we have assigned as $[\text{LRuO}_2(\text{OH})]^+$ **4** (Figure 3). Detection of this dioxo-Ru(VI) species is consistent with the mechanism of Che and co-workers that a dioxo-adduct is the active hydroxylating agent.¹² In addition to **4**, we were able to identify a second dioxo complex, $[\text{LRuO}_2]^+$ **5** (Figure 3). Subjecting $[\text{LRuO}_2]^+$ **5** to collision induced dissociation (CID) requires a relative collision energy of 20% to fragment the ligand. Subjecting $[\text{LRuO}_2(\text{OH})]^+$ to CID, however, leads to loss of H_2O at a relative energy of 10%, which can be attributed to loss of the OH-group and fragmentation of the ligand. Further experiments

without the application of external voltage demonstrated that the composition of the spectrum did not change; applying a 5 kV potential to the syringe supplying the spray resulted in increased overall signal intensity.¹³ To determine the origin of the oxo-groups, ^{18}O -labelled H_2O was employed as solvent. Corresponding mass shifts of 6 Da for $[\text{LRuO}_2(\text{OH})]^+$ **4** and 4 Da for $[\text{LRuO}_2]^+$ **5** were recorded. These data confirm that the oxygen ligands present in these ions either originate from or are rapidly exchanged with solvent under these conditions.¹⁴

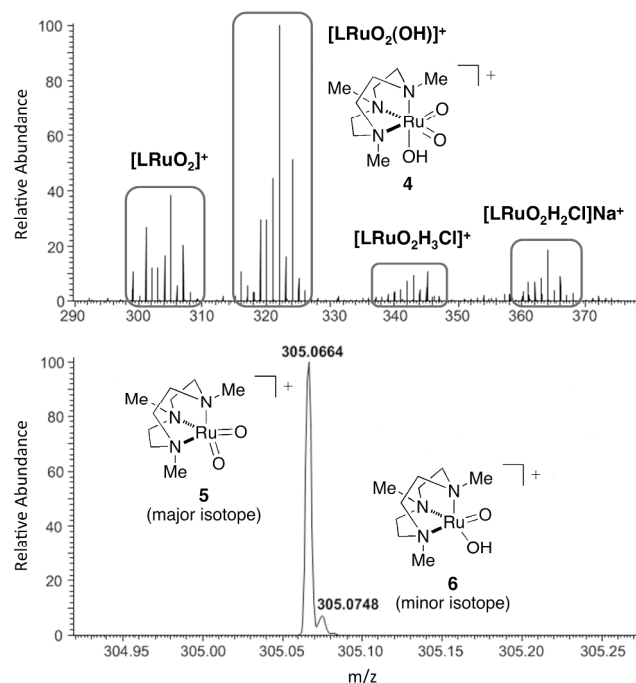


Figure 3. Top: DESI mass spectrum of $[(\text{Me}_3\text{tacn})\text{RuCl}_3]$, pre-treated with AgClO_4 , and substrate **2** sprayed with NaIO_4 . For full spectrum see Figure S4. Bottom: Zoom-in of the signal corresponding to $[\text{LRuO}_2]^+$ and proposed structures for both metal-oxo species. The main isotope of $[\text{LRuO}(\text{OH})]^+$ **6** is at m/z 306.0755.

Upon further analysis of the signal corresponding to $[\text{LRuO}_2]^+$ **5**, a third ruthenium-containing species was identified with a $\Delta m/z$ of +1 Da. While this peak is low intensity, it is well resolved by the Orbitrap MS (set to 60,000 at m/z 400). This new species has one additional hydrogen compared to $[\text{LRuO}_2]^+$ and has been assigned as a mixed hydroxy-oxo-Ru (IV) adduct **6** (Figure 3, bottom). To verify this result, experiments were repeated using different types of surfaces to spot the sample (paper, glass or PTFE), with and without the application of voltage. Signals corresponding to **5** and **6** appear in the spectrum irrespective the experimental conditions. Analogous data were recorded when $[(\text{Me}_3\text{tacn})\text{RuBr}_3]$ was used in place of **1** (Figure S5) While the formation of a mono-oxo Ru (IV) was unexpected, complexes of this type have been previously characterized.¹⁵ In one example, Che has described the synthesis of a $(\text{Me}_3\text{tacn})(\text{bipyridine})\text{Ru(IV)-oxo}$ species, which is capable of oxidizing benzylic and aromatic C–H bonds.¹⁶ Our DESI-MS experiments establish that the combination of $[(\text{Me}_3\text{tacn})\text{RuCl}_3]$, AgClO_4 , and NaIO_4 is capable of generating at least three discrete oxidized ruthenium intermediates. While it is possible that the dioxo-

Ru(VI) adduct **4** functions as the reactive hydroxylating agent, substrate oxidation by Ru(V) **5** and/or Ru(IV) **6** species cannot be discounted at this time.

Due to the nature and number of oxidized ruthenium adducts detected in the DESI-MS spectra, we were interested in examining the relationship between oxidant concentration and catalyst speciation. Varying concentrations of NaIO₄ were sprayed onto a mixture of [(Me₃tacn)RuCl₃], pre-incubated with AgClO₄, and substrate **2**. Figure 4 shows that the intensity of the Ru(III) species [(Me₃tacn)RuO₃H₄]⁺ decreases with increasing concentrations of oxidant. Both **5** and **6** show a maximum intensity at higher oxidant concentrations. The maximum signal for **6** is recorded at [NaIO₄] of 10⁻⁵ M. By contrast, **5** has a signal maximum at an oxidant concentration of 10⁻⁴ M. These results suggest that conversion of **6** to **5** may be occurring at higher periodate concentrations. Above 10⁻⁴ M [NaIO₄], the principal ruthenium species are in the dioxo form (i.e., **4** and **5**).

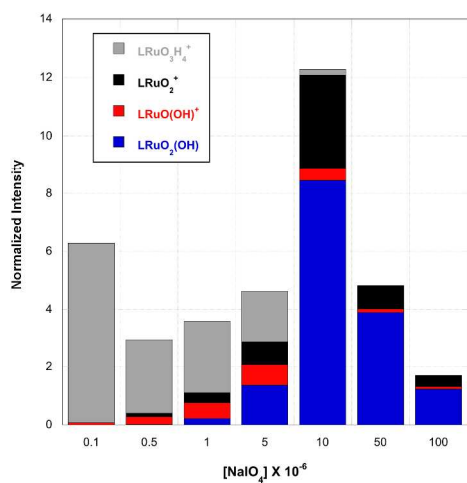


Figure 4. Ruthenium speciation at varying NaIO₄ concentrations. Ion intensities were normalized to the total ion count (TIC) of all ruthenium containing species.

B. Catalytic Turnover and Catalyst Arrest. Our inability to improve yields of C–H hydroxylation products by increasing [(Me₃tacn)RuCl₃] loading has prompted experiments to understand mechanisms for catalyst arrest.¹⁷ The formation of oxo-bridged diruthenium species may be one pathway for catalyst inactivation.¹⁸ We have performed DESI-MS analysis of reaction mixtures following a 24 h mixing period of catalyst **1**, substrate **2**, AgClO₄, and NaIO₄. The reaction mixture was partitioned between aqueous and ethereal solvents, and the contents of each fraction were analysed separately. The full spectrum of the aqueous extract shows the complex composition of the spent mixture (Figure 5).

Analysing the signals that contain at least one ruthenium ion, we have found that all such compounds are in the mass range of 250–650 m/z. After 24 hours, no oxo- or dioxo-derived species can be identified. Notably, these experiments reveal a trioxo-bridged ruthenium dimer, [(Me₃tacn)RuO₃Ru(Me₃tacn)]⁺² **7**, which is detected as a doubly charged species (Figure 5). We believe that dimer formation represents at least one of multiple pathways for inhibition of catalyst turnover. Accordingly, when a solution of

NaIO₄ (5 × 10⁻⁴ M) was sprayed onto a sample of the spent reaction mixture, the MS spectrum did not show any increase in the intensity of hydroxylation products (Figure S6). These results suggest that the ruthenium species present at the end of the reaction, which includes dimer **7**, are no longer active as C–H hydroxylation catalysts. A full list of identified m/z signals, including a variety of mononuclear ruthenium species, is given in Figures S7 and S8. The [(Me₃tacn)RuBr₃] yields similar decomposition products as the [(Me₃tacn)RuCl₃] catalyst (see Figure S9), including the trioxo-bridged dimer.

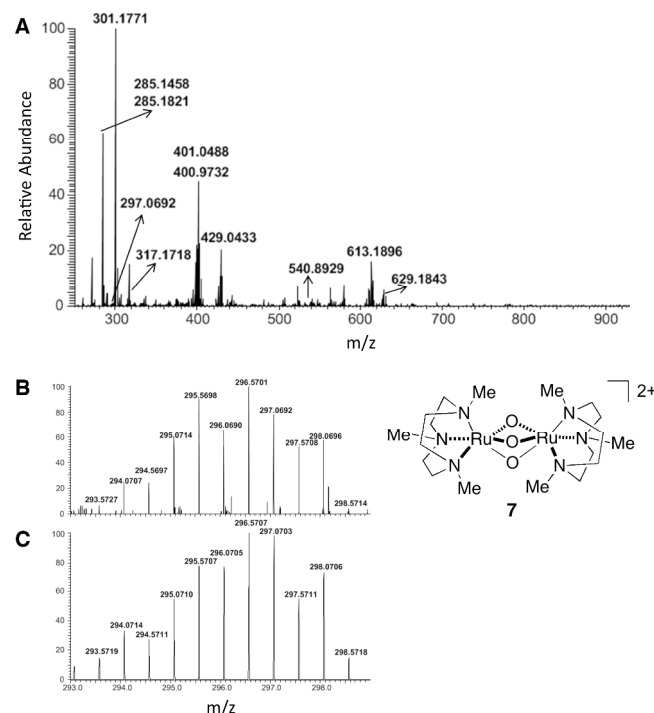
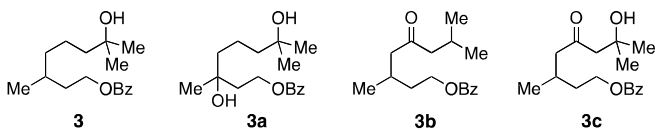


Figure 5A. DESI-Mass spectrum of the aqueous fraction following work-up of a spent reaction mixture (catalyst **1**, AgClO₄, **2**, and NaIO₄, 24 h). **B.** Experimental spectrum showing an isotope profile consistent with trioxo-bridged ruthenium dimer **7**. **C.** Simulated spectrum of **7** (note: 0.5 m/z intervals between isotopes are consistent with the assignment of a dimer having a net dipoisitive charge).

Mass spectral analysis of the ethereal extract of the spent mixture from a reaction with [(Me₃tacn)RuCl₃] is shown in Figure S10. In addition to the major product **3**, five byproducts derived from **2** can be identified (Table 1). These include the bis-diol product **3a** resulting from hydroxylation at both tertiary sites (i.e., C3 and C7) as well as two ketone products that stem from oxidation at any one of the four unsubstituted methylene centers (**3b**, **3c**). Two additional products, **3d** and **3e**, arise from oxidative C–C bond cleavage (possibly through an alkene intermediate). To confirm the chemical formula assignments of the reaction products, a d₅-benzoate-labeled substrate was synthesized. Oxidation of this compound leads to a 5 Da mass shift for the mono-hydroxylated product and all other substrate-derived byproducts (Figure S10). Finally, examination of the product distribution over time (Table 2) shows that the reaction is effectively complete at 3 hours. These data also demonstrate that, as the reaction proceeds, the ruthenium trioxo-ruthenium dimer **7** is formed.

Table 1. Major and minor byproducts from C–H hydroxylation catalysed by **1**. Structures shown for compounds **3b** and **3c** are representative isomers and have not been definitively assigned. Compounds **3d** and **3e** are products arising from C–C bond cleavage.



Entry	Sum formula	m/z	Relative signal intensity
3	[C ₁₇ H ₂₆ O ₃] ⁺ Na ⁺	301.1774	100%
3a	[C ₁₇ H ₂₆ O ₄] ⁺ Na ⁺	317.1723	4.5%
3b	[C ₁₇ H ₂₄ O ₃] ⁺ Na ⁺	299.1618	17.5%
3c	[C ₁₇ H ₂₄ O ₄] ⁺ Na ⁺	315.1567	2.5%
3d	[C ₁₆ H ₂₂ O ₃] ⁺ Na ⁺	285.1461	10.5%
3e	[C ₁₆ H ₂₀ O ₄] ⁺ Na ⁺	299.1254	3.0%

In bulk solution, [(Me₃tacn)RuBr₃] is less effective than [(Me₃tacn)RuCl₃] as a pre-catalyst for C–H hydroxylation of **1**, and affords only 20% of **3** at 2 mol% loading. When the reaction with [(Me₃tacn)RuBr₃] is examined by DESI-MS (24 h), the signal corresponding to substrate **2** (m/z 285.18) is significantly more intense than that of the product **3** (m/z 301.17, Figure 6a). This finding is consistent with the bulk solution data, and contrasts rather markedly the DESI-MS spectrum of a reaction with [(Me₃tacn)RuCl₃]. Using DESI-MS to assess the kinetic profile of the reaction progress clearly demonstrates the superiority of the [(Me₃tacn)RuCl₃] catalyst (Figure 6b). In spite of the presence of Ag(I), clearly the counterion (Cl vs Br) exerts a significant effect on both the speciation of the catalyst and its performance.

Table 2. Changes in the signal intensities (normalized) vs. time of selected ions.

Time (h)	Substrate 2	Product 3	Dimer 7
0.15	162	7	0
0.5	68	43	0
3	55	106	1.72
24	57	108	1.65

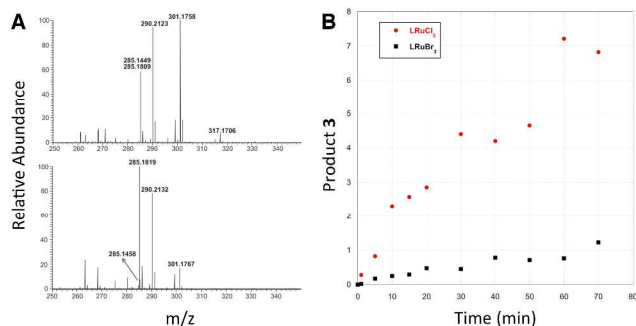


Figure 6 A. Incubated reaction mixtures of (top) [(Me₃tacn)RuCl₃] versus (bottom) (Me₃tacn)RuBr₃. The signals at m/z 301.17, 317.17, 285.18, and 285.14 correspond to the following products: alcohol **3**, diol **3a**, substrate **2**, ketone **3b** or **c**, respectively. The signal at m/z 290.21 is an internal standard. **B.** A plot of product **3** formation vs. time for a reaction catalysed by [(Me₃tacn)RuCl₃] (red) and [(Me₃tacn)RuBr₃] (black).

Conclusions

Our studies have focused on the identification of the active oxidants and potential arrest mechanisms in the [(Me₃tacn)RuCl₃]-catalysed hydroxylation of tertiary C–H bonds. Comparative experiments with [(Me₃tacn)RuBr₃] have also been obtained, and reveal striking differences between these two catalysts, which is reflected in their disparate performance in solution. The power of DESI-MS to detect reaction intermediates and products within milliseconds following initiation is a considerable advantage of this analytical technique. Data from these experiments have raised unforeseen questions regarding the structure(s) of the active oxidant in this Ru-catalysed process. Future efforts to develop next-generation Ru systems for C–H hydroxylation may consider ligand designs that bias generation of a single oxidizing species. In addition to these findings, DESI-MS data has given evidence that catalyst dimerization, in this case to form a trioxo-bridged complex, is deleterious to catalyst turnover. The design of alternative ligand-metal complexes and/or discovery of reaction conditions that can mitigate these second order processes could result in significant boosts in reaction performance.

Experimental Section

The synthesis of the ligand Me₃tacn (1,4,7-trimethyl-1,4,7-triazacyclo-nonane) is described in detail elsewhere.¹⁹ [(Me₃tacn)RuCl₃] was obtained by metalation of 40 μL Me₃tacn with 199 mg [RuCl₂(dmsO)₄] in 1.0 mL ethanol followed by refluxing in concentrated HCl.²⁰ [(Me₃tacn)RuBr₃] was synthesized accordingly using RuCl₂(dmsO)₄ as the starting material and refluxing in HBr. Activation of the catalyst was carried out by dissolving 2 mg the Ru complex in 0.5 mL H₂O and sonicating until fully dissolved. 5 mg AgClO₄ (Sigma-Aldrich) was added and the mixture stirred at 80 °C for 6 min. The heterogeneous mixture was cooled to room temperature, filtered through a cotton plug, and the mass analysed. For the analysis of incubated reaction mixtures, the suspension was transferred into a vial containing 37 mg substrate **2** and 85 mg NaIO₄. The contents were stirred for a prescribed amount of time (10 min, 30 min, 3 h, 24 h), then filtered through a cotton plug. The aqueous fraction was extracted with 3 x 1 mL of Et₂O. DESI-MS experiments were carried out using a homebuilt DESI source (described in S1) coupled to an LTQ-XL Orbitrap mass spectrometer (Thermo Scientific). The instrument parameters were set as follows: temperature inlet capillary: 200 °C; resolution: 60,000 at m/z 400; scan range: 50–1000 m/z; voltage applied to syringe: 5 kV.

Acknowledgements

We gratefully acknowledge financial support from the National Science Foundation under the CCI Center for Selective C–H Functionalization (CHE-1205646). We would like to thank Jialing Zhang for help with DESI-MS experiments. J.L.R. was supported as a Ruth Kirschstein NIH postdoctoral fellow (5F32GM089033). C.F. and J.L.R. thank the Center for Molecular Analysis and Design at Stanford University (CMAD) for postdoctoral fellowship support.

Notes and references

Department of Chemistry, Stanford University, Stanford CA 94305, USA

[†]Present address: Department of Chemistry, Duke University 3236 French Science Center, 124 Science Drive Durham, NC 27708.

†Electronic Supplementary Information (ESI) available: [details of any supplementary information available should be included here]. See DOI: 10.1039/b000000x/

- For general reviews on C–H hydroxylation, see: a) Newhouse, T.; Baran, P. B. *Angew. Chem. Int. Ed.* **2011**, *50*, 3362–3374; b) White, M. C. *Science* **2012**, *335*, 807–809; c) Thirunavukkasrasu, V. S.; Kozhushkov, S. I.; Ackerman, L. *Chem. Commun.* **2014**, *50*, 29–39; d) Company, A.; Lloret, J.; Gomez, L.; Costas, M. *Alkane C–H Activation by Single-Site Metal Catalysis*. Springer Netherlands;
- For examples of non-metal catalysed C–H hydroxylation, see: a) Brodsky, B. H.; Du Bois, J. *J. Am. Chem. Soc.* **2005**, *127*, 15391–15393; b) Litvinas, N. D.; Brodsky, B. H.; Du Bois, J. *Angew. Chem. Int. Ed.* **2009**, *48*, 4513–4516. c) Adams, A. M.; Du Bois, J. *Chem. Sci.* **2014**, *5*, 656–659.
- For examples with stoichiometric oxidants, see: a) Curci, R.; D'Accolti, L.; Fusco, C. *Acc. Chem. Res.* **2006**, *39*, 1–9 and references therein; b) Chen, K.; Richter, J. M.; Baran, P. S. *J. Am. Chem. Soc.* **2008**, *130*, 7247–7249; c) Chen, K.; Baran, P. S. *Nature*, **2009**, *459*, 824–828.
- For recent examples of transition-metal catalysed C–H hydroxylations, see: a) Kim, C.; Chen, K.; Kim, J.; Que Jr., L. *J. Am. Chem. Soc.* **1997**, *119*, 5964–5965; b) Lee, S.; Fuchs, P. L. *J. Am. Chem. Soc.* **2002**, *124*, 13978–13979; c) Chen, M. S.; White, M. C. *J. Am. Chem. Soc.* **2004**, *126*, 1346–1347; d) Lee, S.; Fuchs, P. L. *Org. Lett.* **2004**, *6*, 1437–1440; e) Dick, A. R.; Hull, K. L.; Sanford, M. S.; *J. Am. Chem. Soc.* **2004**, *126*, 2300–2301; f) Chen, M. S.; White, M. C. *Science* **2007**, *318*, 783–787; g) Company, A.; Gomez, L.; Fontrodona, X.; Ribas, X.; Costas, M.; *Chem. Eur. J.* **2008**, *14*, 5727–5731; h) Vermeulen, N. A.; Chen, M. S.; White, M. C. *Tetrahedron*, **2009**, *65*, 3078–3084; i) Zhang, Y.-H.; Yu, J.-Q. *J. Am. Chem. Soc.* **2009**, *131*, 14654–14655; j) Chen, M. S.; White, M. C. *Science* **2010**, *327*, 566–571; k) Company, A.; Prat, I.; Frisch, J. R.; Mas-Balleste, R.; Guell, M.; Juhasz, G.; Ribas, X.; Munck, E.; Luis, J. M.; Que Jr., L.; Costas, M. *Chem. Eur. J.* **2011**, *17*, 1622–1634; l) Prat, I.; Mathieson, J. S.; Guell, M.; Ribas, X.; Luis, J. M.; Cronin, L.; Costas, M.; *Nat. Chem.* **2011**, *3*, 788–793. m) McNeill, E.; Du Bois, J. *J. Am. Chem. Soc.* **2010**, *132*, 10202–10204.
- McNeill, E.; Du Bois, J. *Chem. Sci.* **2012**, *3*, 1810–1813.
- a) Takáts, Z.; Wiseman, J. M.; Gologan, B.; Cooks, R. G. *Science* **2004**, *306*, 471–473. b) Takáts, Z.; Wiseman, J. M.; Cooks, R. G. *J. Mass Spectrom.* **2005**, *40*, 1261–1275.
- a) Vikse, K. L.; Ahmadi, Z.; Manning, C. C.; Harrington, D. A.; McIndoe, J. S. *Angew. Chem. Int. Ed.* **2011**, *50*, 8304–8306; b) Coelho, F.; Eberlin, M. N. *Angew. Chem. Int. Ed.* **2011**, *50*, 5261–5263; c) Zhu, L.; Gamez, G.; Chen, H. W.; Huang, H. X.; Chingin, K.; Zenobi, R. *Rapid Commun. Mass Spec.* **2008**, *22*, 2993–2998; d) Ingram, A. J.; Solis-Ibarra, D.; Zare, R. N.; Waymouth, R. H.; *Angew. Chem. Int. Ed.* **2014**, in press.
- a) Johansson, J. R.; Norden, B. *Proc. Nat. Acad. Sci.* **2012**, *109*, 2186–2187; b) Perry, R. H.; Brownell, K. R.; Chingin, K.; Cahill, T. J.; Waymouth, R. M.; Zare, R. N. *Proc. Nat. Acad. Sci.* **2012**, *109*, 2246–2250; c) Perry, R. H.; Cahill, T. J.; Roizen, J. L.; Du Bois, J.; Zare, R. N. *Proc. Nat. Acad. Sci.* **2012**, *109*, 18295–18299. d) Gouré, E.; Avenier, F.; Dubourdeaux, P.; Sénèque, O.; Albrieux, F.; Lebrun, C.; Clémancey, M.; Maldivi, P.; Latour, J.-M. *Angew. Chem. Int. Ed.* **2014**, *53*, 1580–1584.
- Perry, R. H.; Splendore, M.; Chien, A.; Davis, N. K.; Zare, R. N. *Angew. Chem. Int. Ed.* **2011**, *50*, 250–254.
- Perry, R. H.; Cooks, R. G.; Noll, R. J. *Mass Spectrom. Rev.* **2008**, *27*, 661–699.
- DESI-MS spectra were analogous for experiments performed with either ceric ammonium nitrate (CAN) or NaIO₄. NaIO₄ showed reduced ion suppression at higher concentrations and was therefore preferred for these studies.
- a) Chan, S. L. F.; Kan, Y. H.; Yip, K. L.; Huang, J. S.; Che, C.-M. *Coord. Chem. Rev.* **2011**, *255*, 899–919. b) Cheng, W. C.; Yu, W. Y.; Cheung, K. K.; Che, C.-M. *J. Chem. Soc., Chem. Comm.* **1994**, 1063–1064.
- These data rule out the possibility that oxo-adducts originate from the electrospray process, see: Pasilis, S. P.; Kertesz, V.; Van Berkel, G. J. *Anal. Chem.* **2008**, *80*, 1208–1214. In addition, no Ru-oxo species are detected when experiments are performed in the absence of NaIO₄.
- For examples of H₂O¹⁸ exchange with Ru-oxo species, see: Wang, C.; Shalyaev, K. V.; Bonchio, M.; Carofiglio, T.; Groves, J. T. *Inorg. Chem.* **2006**, *45*, 4769–4782.
- a) Che, C.-M.; Ho, C.; Lau, T.-C. *J. Chem. Soc., Dalton Trans.* **1991**, 1901–1907. b) Cheng, W.-C.; Yu, W.-Y.; Zhu, J.; Cheung, K.-K.; Peng, S.-M.; Poon, C.-K.; Che, C.-M.; *Inorg. Chim. Acta.* **1996**, *242*, 105–113. c) Yu, W.-Y.; Fung, W.-H.; Zhu, J.-L.; Cheung, K.-K.; Ho, K.-K.; Che, C.-M. *J. Chin. Chem. Soc.* **1999**, *46*, 341–349.
- Cheng, W.-C.; Yu, W. Y.; Cheung, K. K.; Che, C.-M. *J. Chem. Soc., Dalt. Trans.* **1994**, 57–62.
- E. McNeill, Ph.D Thesis, Stanford University, 2012.
- a) Garcia-Bosch, I.; Company, A.; Cady, C. W.; Styring, S.; Browne, W. R.; Ribas, X.; Costas, M. *Angew. Chem. Int. Ed.* **2011**, *50*, 5647–5652; b) Gomez, L.; Garcia-Bosch, I.; Company, A.; Benet-Buchholz, J.; Polo, A.; Sala, X.; Ribas, X.; Costas, M. *Angew. Chem. Int. Ed.* **2009**, *48*, 5720–5723.
- Wiegardt, K.; Chaudhuri, P.; Nuber, B.; Weiss, J. *Inorg. Chem.* **1982**, *21*, 3086–3090.
- Neubold, P.; Della Vedova, B. S. P. C.; Wiegardt, K.; Nuber, B.; Weiss, J. *Inorg. Chem.* **1990**, *29*, 3355–3363.